AIMS Mathematics, 8(2): 3542–3560.
DOI: 10.3934/math.2023180
Received: 26 June 2022
Revised: 12 October 2022
Accepted: 12 October 2022
Published: 22 November 2022

http://www.aimspress.com/journal/Math

Research article

An exact solution of heat and mass transfer analysis on hydrodynamic magneto nanofluid over an infinite inclined plate using Caputo fractional derivative model

J. Kayalvizhi[1], A. G. Vijaya Kumar[1,*], Ndolane Sene[2], Ali Akgül[3,4,*], Mustafa Inc[5,6,*], Hanaa Abu-Zinadah[7] and S. Abdel-Khalek[8]

[1] Department of Mathematics, School of Advanced Sciences Vellore Institute of Technology, Vellore-632014, India
[2] Department of Mathematics, Institut des Politiques Publiques, Cheikh Anta Diop University, Dakar Fann, Senegal
[3] Siirt University, Art and Science Faculty, Department of Mathematics, 56100 Siirt, Turkey
[4] Near East University, Mathematics Research Center, Department of Mathematics, Near East Boulevard, PC: 99138, Nicosia/Mersin 10-Turkey
[5] Department of Mathematics, Science Faculty, Firat University, 23119 Elazig, Turkey
[6] Department of Medical Research, China Medical University, 40402 Taichung, Taiwan
[7] University of Jeddah, College of Science, Department of Statistics, Jeddah, Saudi Arabia
[8] Department of Mathematics, College of Science, Taif University, P.O. Box 11099, Taif 21944, Saudi Arabia

* **Correspondence:** Email: vijayakumarag@vit.ac.in, aliakgul@siirt.edu.tr, minc@firat.edu.tr.

Abstract: This paper presents the problem modeled using Caputo fractional derivatives with an accurate study of the MHD unsteady flow of Nanofluid through an inclined plate with the mass diffusion effect in association with the energy equation. H_2O is thought to be a base liquid with clay nanoparticles floating in it in a uniform way. Bousinessq's approach is used in the momentum equation for pressure gradient. The nondimensional fluid temperature, species concentration, and fluid transport are derived together with Jacob Fourier sine and Laplace transforms Techniques in terms of exponential decay function, whose inverse is computed further in terms of Mittag-Leffler function. The impact of various physical quantities interpreted with fractional order of the Caputo derivatives. The obtained temperature, transport, and species concentration profiles show behaviours for $0 < \alpha < 1$ where α is the fractional parameter. Numerical calculations have been carried out for

the rate of heat transmission and the Sherwood number is swotted to be put in the form of tables. The parameters for the magnetic field and the angle of inclination slow down the boundary layer of momentum. The distributions of velocity, temperature, and concentration expand more rapidly for higher values of the fractional parameter. Additionally, it is revealed that for the volume fraction of nanofluids, the concentration profiles behave in the opposite manner. The limiting case solutions also presented on flow field of governing model.

Keywords: nanofluid; heat and mass transfer; magnetic field; Caputo fractional derivative; Fourier and integral transforms
Mathematics Subject Classification: 35Q30, 26A33

Abbreviations:

Nomenclature

B_0	Magnetic field strength
V	Velocity
T	Temperature
C	Concentration
T_∞	Ambient temperature
M	Magnetic parameter
Gr	Grashof number
Gm	Mass of Grashof number
Nu	Nusselt number
Pr	Prandtl number
α	Fractional parameter
γ	Inclined angle
D	Diffusion
Sc	Schimidt number

Greek symbols

β	Thermal expansion
μ	Viscosity
ρ	Density
σ	Electrical conductivity
ϕ	Volume fraction of nanoparticles
$(\rho c_p)_{hnf}$	Heat capacity of the hybrid nanofluid
$(\rho c_p)_f$	Heat capacity of the fluid
$(\rho c_p)_s$	Heat capacity of the nanoparticles material
k_{hnf}	Thermal conductivity of the hybrid nanofluid

μ_{hnf}	Viscosity of hybrid nanofluid
γ_f	fluid kinematic viscosity

Subscripts

f	Fluid
hnf	Hybrid nanofluid
s	Solid particle
w	Condition at the sheet
∞	Ambient conditions

1. Introduction

The importance of nanotechnology is enhancing the heat capacity of liquids by increasing heat and mass transport rates is gaining prominence. The issue of nanofluids has been a broader issue for the academic community in recent years because of their wide variety of applications in heat exchangers, biomedicine, electrical device cooling, double windowpane, food, transportation, and other sectors. We must add different kinds of nanoparticles to the base fluids, such as graphene, silica, silver, gold, copper, alumina, carbon nanotubes, and so on, to boost the heat capacity of common fluids like water, kerosene, and motor oils. Choi and Eastman [1] were the first to introduce these nanofluids. A vast number of research papers dealing with enhancing the heat conductivity of base liquids by accumulating different kinds of nanoparticles have been published in the literature. Wong et al. [2] covered a wide range of nanofluid uses. To make nanofluids easier to understand, Mohain et al. [3] provided the critical thinking and fresh innovations. A comprehensive elucidation of thermophysical properties and an accurate simulation of heat transfer in nanofluid flow were the main points of focus for the researchers. Eastman et al. [4,5] reported that when CuO nanoparticles with a volume fraction of 5% are introduced to the base fluid (water), the heat conduction of the considered base fluid increases at most 0.6. Whereas 1% of copper nanoparticles was introduced into ethylene glycol or oil, 40% thermal conductivity was increased. This is due to metals having three times the thermal conductivity of general fluids. This permits to carry out heat transmission with a mix up of two constituents that act as a fluid matter but possess the thermal conductivity of metals.

The study of magnetohydrodynamics coupled with heat and mass transport has captured the interest of many academics due to its wide range of applications. Due to the many different fields that MHD may be used in, including biomedical engineering, geophysics, magnetic drug targeting, engineering, and many more, there has been a lot of interest in the field in recent years. Employing Caputo fractional derivatives, a Brinkman-type fluid flow with mass transfer in an unstable MHD flow was examined by N. A. Sheikh et al. [6,7]. A Maxwell fluid with correlated effects of heat and mass transport is investigated by M. M. Ghalib et al. [8] under slip and non-slip boundary conditions. With the concept of non-integer order derivatives, N. Iftikhar et al. [9] examine the MHD Oldroyd-B fluid. An angled magnetic force Casson nanofluid based on kerosene oil and water was studied by A. Raza et al. [10].

In the past 10 years, fractional derivatives have been used to represent a wide variety of practical events. Fractional calculus is a rapidly expanding discipline in the contemporary period due to its wide-ranging consequences in a variety of real-world occurrences such as in electromagnetism,

modelling in biological, biomedical and epidemic problems, dynamical behaviour of fluid matters, wave traveling solutions, signals processing, economics and viscoelastic behaviour of fluids are few examples of fractional calculus applications. Many academics have recently come to the conclusion that fractional derivatives provide more reliable and accurate findings than ordinary derivatives. This is because an acceptable fractional parameter adaptation results in almost complete congruence between theoretical and experimental assessments. Some rheological properties of fluids can only be seen using fractional derivatives in the subject of fluid mechanics. As a result, scientists realized that generating unique fractional derivatives with distinct benefits over regular derivatives was critical in confirming a few specifications in modeling computational and mathematical problems. To date, all fractional derivatives presented use a unique kernel. Leibnitz and L. Hospital are credited with doing the foundational work on the fractional order technique in the year 1695 [11]. Fractional operators in biological modelling are examined as a broad topic [12] in their physical model [13], in the investigations of mathematical physics [14,15], in applications of mathematics [16]. There are a great number of fractional derivatives, and they each offer some distinct benefits.

The Riemann-Liouville derivative and the integral associated with it are both considered to be fractional operators. The Caputo-Fabrizio derivative as well as the integral that is connected with it. The usefulness of Fractional calculus has been extensively studied in the scientific literature [17]. For the flow problems, academics as F. Ali et al. [18,19], apply the fractional derivatives technique. Caputo-Fabrizio fractional derivatives [20] are another way of representing fractional derivatives; they are sometimes referred to in the literature as derivatives with a non-singular kernel. The use of fractional derivatives by Atangana and Koca [21] demonstrated the existence and uniqueness of a solution to the issue. The Riemann-Liouville integral operator and Mittag-Leffler functions have been developed numerically by Diehelm and coworkers [22]. Using fractional derivatives, S. Aman et al. [23] attempt to obtain an accurate solution to the flow field, fluid temperature, and species levels of a forced convective flow of graphene nanofluid prepared by graphene nanoparticles in an ambient stream of upright surface. A viscous fluid with a heat/sink was studied over an upright cylinder by considering a combination of 47 nm alumina nanoparticles in water as a heat source has been given by N. A. Shah et al. [24]. In [25], A. Raza et al. have conducted research on the exact solutions of fractional nanofluids moving on an endless surface at a fixed temperature while accounting for heat flux and radiation impact. M. D. Ikram et al. [26] estimated hybrid nanoparticles suspended in Brinkman type fluid (BTF) have been explored using a fractional fractional model. The majority of the research concentrated on fluid flow issues by examining various liquids, connected to fractional order derivatives, and in the process of heat transmission. Some pertinent works with subject to fractionalized models are discovered in depth [27–30]. H. Elhadedy et al. [31] used the ρ-Laplace transform and finite sin-Fourier transform to solve fractional differential equations with a generalized Caputo derivative. They employ these transformations to solve the time-fractional heat equation using a generalized Caputo fractional derivative. Fractional heat equation on a spherical domain with a hybrid fractional derivative operator is studied by A. H. A. Kader et al. [32].

Using fractional calculus, M. Khan et al. [33] examined modeling charge carrier transport with anomalous diffusion and heat conduction in amorphous semiconductors. M. Irfan et al. [34] evaluated the effectiveness of a novel mass flux theory on Carreau nanofluid employing thermal aspects of convective heat transfer with nonlinear properties of mixed convection. I. Ali et al. [35] describe the phase dynamics of an inline long Josephson junction in a voltage state under the effect of a constant external magnetic field. A fractional calculus technique is utilized to simulate the growth of the phase difference between the macroscopic wave functions of the two superconductors

across the junction. The stagnation point in Jeffery liquid flow through a deformable cylinder is investigated by Z. Hussain et al. [36] a Cattaneo-Christov model with double stratification, heat source, and thermal relaxation is used to examine heat and mass transmission. N. S. Akbar et al. [37] studied the effects of an external magnetic field and gravity on the stable incompressible flow of a temperature-dependent viscous nanofluid flowing from a vertically stretched sheet. The benefits of applying the fractional calculus theory to many scientific and engineering fields: 1) tuning of PID controllers using fractional calculus concepts; 2) fractional PD^{α} control of a hexapod robot; 3) fractional dynamics in the trajectory control of redundant manipulators; 4) circuit synthesis using evolutionary algorithms; 5) heat diffusion.

In the present work, the resulting flow of governing equations is translated into fractional PDEs and solved utilizing a combination of Fourier series and the Laplace Transform Technique. The computational results were obtained through MATLAB with the help of Euler-inversion. It can be seen that the influence of some flow quantities and the order of the fractional parameter α on the fluid velocity, temperature, and species concentration analysed graphically in the proposed research work.

2. Mathematical formulation

We address the unsteady flow of an incompressible MHD viscous nano fluid through an infinite inclined plate with mass and heat transfer through the caputo fractional derivative. y axis is taken along the plate with an angle of inclination to the vertical, while the x axis is normal to the plate. In the x direction, a uniform magnetic field is applied transversely to the plate as shown in Figure 1. The xy-plane filled with nanofluid contains Clay nanoparticles. Fluid is flowing in the y direction along with the inclined plate. Initially $(t' = 0)$ the plate surface and nanofluids are static condition and after a certain time $t' > 0$, the plate moves with velocity U and at the same time its temperature raises to T_w. The buoyant force is the essential mechanism in driving the fluid though gravity is pulling down the fluid flow. Since the plate is taken at an infinite length, the boundary layer thickness is considerably small when compared, hence all the flow fields are only function of one special coordinate and with respect to time. The governing equations of momentum, energy, and concentration describing the fluid flow phenomena are formulated accordingly to simplify pressure gradient and body force in the Navier-Stokes equation and presented in dimensionless form with Caputo fractional derivative as follows [38,39]:

$$\rho_{nf}\frac{\partial^{\alpha}\, \mathrm{v}'(\mathrm{x},\mathrm{t})}{\partial t'^{\alpha}} = \mu_{nf}\frac{\partial^2 v'}{\partial x'^2} + (\rho g_T)_{nf}\left(T'-T'_{\infty}\right)\cos\gamma + (\rho g_C)_{nf}\left(C'-C'_{\infty}\right)\cos\gamma - \sigma_{nf}B^2 v', \tag{1}$$

$$(\rho_{cp})_{nf}\frac{\partial^{\alpha} T'(\mathrm{x},\mathrm{t})}{\partial t'^{\alpha}} = K_{nf}\frac{\partial^2 T'}{\partial x'^2}, \tag{2}$$

$$\frac{\partial^{\alpha} C'(\mathrm{x},\mathrm{t})}{\partial t'^{\alpha}} = D_{nf}\frac{\partial^2 C'}{\partial x'^2}, \tag{3}$$

with appropriate initial and boundary conditions [39],

$$v(x,0) = 0,\ T(x,0) = T_{\infty},\ C(x,0) = C_{\infty}$$

$$v(0,t) = V,\ T(0,t) = T_w, C(0,t) = C_w$$

$$v(\infty,t)\to 0,\ T(\infty,t)\to T_\infty,\ C(\infty,t)\to C_\infty\ .$$

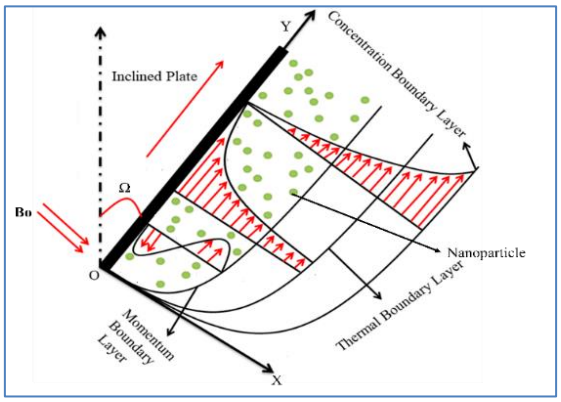

Figure 1. Flow configuration of the problem.

The physical properties of nanofluid provided by [40] as follows:

$$\frac{\mu_{nf}}{(1-\phi)^{2.5}\mu_f}=1,$$

$$\rho_{nf}=(1-\phi)\rho_f+\phi\rho_s,$$

$$knf=k_f\left[\frac{(k_s+2k_f)-2\phi(k_f-k_s)}{(k_s+2k_f)+\phi(k_f-k_s)}\right],$$

$$(\rho cp)_{nf}=(\rho cp)_s\phi+(1-\phi)(\rho cp)_f,$$

$$(\rho\beta)_{nf}=(1-\phi)(\rho\beta)_f+\phi(\rho\beta)_s\ \ ,\ \ \sigma_{nf}/\sigma_f=\left[1+\frac{3(\sigma-1)\phi}{(\sigma+2)-\phi(\sigma-1)}\right].$$

The subscript f denotes base fluids and s denotes nanoparticles, while the subscript ϕ stands for the nanoparticle volume concentration.

To obtain a prototype model, the following non-dimensional parameters are construced with the help of Buckingham's pi-thereom.

$$u'=\frac{u}{v},x'=\frac{U}{\gamma}\mathrm{x},T'=\frac{U^2}{\gamma}t,\theta=\frac{T'-T'_\infty}{T_w{}'-T'_\infty},C=\frac{C'-C'_\infty}{C'_w-C'_\infty},pr=\frac{\mu cp}{k},Gr=\frac{\beta g\gamma(T'_w-T'_\infty)}{{u_0}^3},Gm=\frac{\beta g\gamma(C'_w-C'_\infty)}{{u_0}^3},$$

$$M=\frac{\sigma {B_0}^2}{\rho {u_0}^2}.$$

With the use of these dimensionless numbers, the governing Eqs (1)–(3) and corresponding conditions, once after dropping asterisk can be yield as

$$D_t^\alpha v=a_1\frac{\partial^2 v}{\partial x^2}+a_2Gr\ \cos\Omega\ \theta+a_2Gm\cos\Omega\ \ C-a_4M\,v,\tag{4}$$

$$D_t^\alpha\theta=a3\frac{1}{\mathrm{Pr}}\frac{\partial^2\theta}{\partial x^2},\tag{5}$$

$$\frac{sc}{a_5} D_t^{\alpha} C = \frac{\partial^2 C}{\partial x^2}. \tag{6}$$

Where,

$$z_1 = \left[1-\phi+\phi\frac{(\rho)_s}{(\rho)_f}\right], \quad z_2 = \left[1-\phi+\phi\frac{(\rho\beta)_s}{(\rho\beta)_f}\right],$$

$$z_3 = \left[1-\phi+\phi\frac{(\rho cp)_s}{(\rho cp)_f}\right], \quad z_4 = \left[1+\frac{k_s-2\phi\left(k_f-k_s\right)+2k_f}{k_s+\phi\left(k_f-k_s\right)+2k_f}\right],$$

$$a_1 = \frac{\mu_f}{(1-\phi)^{2.5} z_1}, \quad a_2 = \frac{z_2}{z_1}, \quad a_3 = \frac{z_4}{z_3}, \quad a_4 = \frac{z_5}{z_1}, a_5 = (1-\phi).$$

The boundary conditions are taken into consideration

$$v(x,0) = 0, \theta(x,0) = 0, c(\mathrm{x},0) = 0, \tag{7}$$

$$v(0,\tau) = 1, \theta(0,\tau) = 1, c(0,\tau) = 1. \tag{8}$$

2.1. Solution of the problem

For the fractional differential equations presented in Eqs (4)–(6) various approaches exist for finding their solutions. In the present investigation, both of Integral transforms are employed such as Laplace transform of the Caputo fractional derivative and the Fourier sine transformation for classical derivatives to find the precise results of the governing model.

2.2. Energy equation

From Eq (5) the Fourier sine transformation is applied to the equation, yielding the following relationship:

$$F_s\left[D_\tau^{\alpha}\theta(x,\tau)\right] = \frac{1}{\mathrm{Pr}} a_3 F_s\left[\frac{\partial^2\theta}{\partial x^2}(x,\tau)\right],$$

$$D_\tau^{\alpha}\theta(q,\tau) = \frac{1}{\mathrm{Pr}} a_3\left[q\theta(0,\tau) - q^2\theta(q,\tau)\right]. \tag{9}$$

The next step is the Integral transformation, which involves the integral transform to the Caputo derivative; and once simplifying, we get the following equations:

$$L\left(D_\tau^{\alpha}\theta(q,\tau)\right) = \frac{q}{\mathrm{Pr}} a_3 L\left[\theta(0,\tau)\right] - \frac{q^2}{\mathrm{Pr}} a_3 L\left[\theta(0,\tau)\right],$$

$$\theta(q,s) = \frac{1}{q}\left\{\frac{1}{s} - \frac{S^{\alpha-1}}{S^{\alpha}+\frac{q^2 a_3}{\mathrm{Pr}}}\right\}. \tag{10}$$

After obtaining the above expression derived from energy equation with fractional derivative using the methods outlined in [41] and then using the inverse integral transform, we can get the following form:

$$L^{-1}\left[\theta(q,s)\right]=L^{-1}\left[\frac{1}{q}\left(\frac{1}{s}-\frac{s^{\alpha-1}}{s^{\alpha}+\frac{q^2a_3}{\Pr}}\right)\right].$$

To find the value of $L^{-1}\left(\frac{s^{\alpha-1}}{s^{\alpha}+q^2a_3/\Pr}\right)$ by using Mittag-Leffler function

$$E_{\alpha}\left(-\frac{q^2}{\Pr}\tau^2\right)=L^{-1}\left[\frac{S^{\alpha}-1}{S^{\alpha}+q^2a_3/\Pr}\right],$$

$$\theta(q,\tau)=\frac{1}{q}\left[1-E_{\alpha}\left(-\frac{q^2a_3}{\Pr}\tau^2\right)\right]. \tag{11}$$

As described in [42], we should perform the inverse Fourier transform on Eq (11)

$$\theta(x,\tau)=1-\frac{2}{\pi}\int_0^{\infty}\frac{\sin qx}{q}E_{\alpha}\left(-\frac{q^2a_3}{\Pr}\tau^{\alpha}\right)dq. \tag{12}$$

2.3. Concentration equation

From Eq (6) the Fourier sine transformation is applied to this equation, yielding the following relationship:

$$F_s\left[\frac{sc}{a_5}D_t{}^{\alpha}C\right]=F_s\left[\frac{\partial^2C}{\partial x^2}\right],$$

$$D_{\tau}^{\alpha}c(q,\tau)=\frac{a_5}{sc}\left[qc(0,\tau)-q^2c(q,\tau)\right]. \tag{13}$$

The next step is the Integral transformation, which involves the integral transform to the Caputo derivative; with a rearrangement of terms, we get the following form:

$$L\left[D_{\tau}^{\alpha}c(q,\tau)\right]=\frac{a_5}{sc}L\left[qc(0,\tau)-q^2c(q,\tau)\right],$$

$$c(q,s)=\frac{1}{q}\left\{\frac{1}{s^{\alpha}}-\frac{s^{\alpha-1}}{s^{\alpha}+\frac{q^2a_5}{sc}}\right\}. \tag{14}$$

After determining the above expression to the concentration equation with fractional derivative using

the methods outlined in [41], and then Using the inverse integral transform, we can get the following equation:

$$L^{-1}\left[c(q,s)\right]=\frac{1}{q}L^{-1}\left\{\frac{1}{s^{\alpha}}-\frac{s^{\alpha-1}}{s^{\alpha}+q^{2}a_{5}/sc}\right\}.$$

To find the value of $L^{-1}\left(\frac{s^{\alpha-1}}{s^{\alpha}+q^{2}a_{5}/sc}\right)$ by using Mittag-Leffler function

$$E_{\alpha}\left(-\frac{q^{2}a_{5}}{sc}\tau^{\alpha}\right)=L^{-1}\left[\frac{S^{\alpha}-1}{S^{\alpha}+q^{2}a_{5}/sc}\right],$$

$$c(q,\tau)=\frac{1}{q}\left[1-E_{\alpha}\left(-\frac{q^{2}a_{5}}{sc}\tau^{\alpha}\right)\right]. \tag{15}$$

As described in [42], we should perform the inverse Fourier transform on Eq (15)

$$c(x,\tau)=1-\frac{2}{\pi}\int_{0}^{\infty}\frac{\sin qx}{q}E_{\alpha}\left(-\frac{q^{2}a_{5}}{sc}\tau^{\alpha}\right)dq\,. \tag{16}$$

2.4. Velocity equation

From Eq (4) the Fourier sine transformation is applied to this equation, yielding the following relationship:

$$F_{s}\left[D_{t}^{\alpha}v\right]=F_{s}\left[a_{1}\frac{\partial^{2}v}{\partial x^{2}}+a_{2}Gr\cos\Omega\;\theta+a_{2}Gm\;\cos\Omega\;C-a_{4}Mv\right],$$

$$\begin{aligned}D_{\tau}^{\alpha}v(q,z)=a_{1}qv(0,\tau)-a_{1}q^{2}v(q,\tau)+a_{2}Gr\;\cos\gamma\;\theta(q,\tau)+\\ a_{2}Gm\;\cos\gamma\;C(\mathrm{q},\tau)-\mathrm{a}_{4}\mathrm{M}\,v(q,\tau)\end{aligned}. \tag{17}$$

The second step is the Integral transformation, which involves the integral transform to the Caputo derivative; with rearrangement of terms, we get the following equations:

$$\begin{aligned}L\left[D_{\tau}^{\alpha}v(q,z)\right]=a_{1}qL\left[v(0,\tau)\right]-a_{1}q^{2}L\left[v(q,\tau)\right]+a_{2}Gr\cos\gamma L\left[\theta(q,\tau)\right]+\\ a_{2}\,Gm\;\cos\gamma\;L\left[C(\mathrm{q},\tau)\right]-a_{4}M\,\bar{v}\end{aligned}$$

$$v(q,s)=\frac{a_1 q}{S\left(s^{\alpha}+a_1 q^2\right)}+\frac{Gr\cos\gamma q\, a_2}{\mathrm{spr}\left(s^{\alpha}+q^2/\mathrm{Pr}\right)\left(s^{\alpha}+a_1 q^2\right)}+\frac{Gm\,\cos\gamma q\, a_2}{\mathrm{spr}\left(s^{\alpha}+q^2/\mathrm{Pr}\right)\left(s^{\alpha}+a_1 q^2\right)}-\frac{Ma_4}{\mathrm{spr}\left(s^{\alpha}+q^2/\mathrm{Pr}\right)\left(s^{\alpha}+a_1 q^2\right)},$$

where,

$$a(q,s)=\frac{a_1 q}{s\left(s^{\alpha}+q^2 a_4/\mathrm{Pr}\right)},$$

$$b(q,s)=\frac{q\,Gr\cos\gamma\, a_2}{\mathrm{Pr}\,s\left(s^{\alpha}+q^2 a_4/\mathrm{Pr}\right)\left(s^{\alpha}+a_1 q^2\right)},$$

$$c(q,s)=\frac{q\,Gm\cos\gamma\, a_2}{\mathrm{Pr}\,s\left(s^{\alpha}+q^2 a_4/\mathrm{Pr}\right)\left(s^{\alpha}+a_1 q^2\right)},$$

$$d(q,s)=\frac{Ma_4}{\mathrm{Pr}\,s\left(s^{\alpha}+q^2 a_4/\mathrm{Pr}\right)\left(s^{\alpha}+a_1 q^2\right)}.$$

After obtaining the above expression to the velocity equation with fractional derivative using the methods outlined in [41], further using the inverse Integral transform, we can get the following form:

$$L^{-1}\left[v(q,s)\right]=L^{-1}\left[\frac{a_1 q}{S\left(s^{\alpha}+a_1 q^2\right)}+\frac{Gr\cos\gamma\, q\, a_2}{\mathrm{spr}\left(s^{\alpha}+a_4 q^2/\mathrm{Pr}\right)\left(s^{\alpha}+a_1 q^2\right)}+\frac{Gm\,\cos\gamma\, q\, a_2}{\mathrm{spr}\left(s^{\alpha}+a_4 q^2/\mathrm{Pr}\right)\left(s^{\alpha}+a_1 q^2\right)}-\frac{Mq\, a_4}{\mathrm{spr}\left(s^{\alpha}+a_4 q^2/\mathrm{Pr}\right)\left(s^{\alpha}+a_1 q^2\right)}\right],$$

$$a(q,\tau)=\frac{1}{q}\left[1-E_{\alpha}\left(-a_1 q^2\tau^{\alpha}\right)\right],$$

$$b(q,\tau)=\frac{Gr\cos\Omega\,\tau^{\alpha} a_2}{\mathrm{Pr}\,q\left(a_1-\frac{1}{\mathrm{Pr}}\right)}\left[E_{\alpha,\beta}\left(\frac{-q^2 a_3}{\mathrm{Pr}}\tau^{\alpha}\right)-E_{\alpha,\beta}\left(-a_1 q^2\tau^{\alpha}\right)\right],$$

$$c(\mathrm{q},\tau)=\frac{Gm\,\cos\Omega\,\tau^{\alpha} a_2}{prq(\mathrm{a}_1-\mathrm{pr})}\left[E_{\alpha,\beta}\left(-\frac{q^2 a_3}{pr}\tau^{\alpha}\right)-E_{\alpha,\beta}\left(-\mathrm{a}_1\, q^2\tau^{\alpha}\right)\right],$$

$$\mathrm{d}(\mathrm{q},\tau)=\frac{M\ \tau^{\alpha}a_4}{pr\,q(\mathrm{a}_1-\mathrm{pr})}\left[E_{\alpha,\beta}\left(-\frac{q^2a_3}{pr}\tau^{\alpha}\right)-E_{\alpha,\beta}\left(-\mathrm{a}_1\,q^2\tau^{\alpha}\right)\right],$$

$$v(\mathrm{q},\tau)=\mathrm{a}(\mathrm{q},\tau)+b(\mathrm{q},\tau)+c(\mathrm{q},\tau)-\mathrm{d}(\mathrm{q},\tau). \tag{18}$$

As described [42], we should perform the inverse Fourier transform on Eq (18)

$$a(\mathrm{x},\tau)=1-\frac{2}{\pi}\int_0^{\infty}\frac{\sin qx}{q}E_{\alpha}(-a_1\,\mathrm{q}^2\,\tau^{\alpha})\,\mathrm{dq},$$

$$b\left(x,\tau\right)=\frac{2a_2Gr}{k}\int_0^{\infty}\sin\frac{qx\,\tau^{\alpha}}{q}\left[E_{\alpha,\beta}\left(\frac{-a_3q^2}{\mathrm{Pr}}\tau^{\alpha}-E_{\alpha,\beta}\left(-a_1q^2\tau^{\alpha}\right)\right)\right]\sin qx\,dq,$$

$$c(\mathrm{x},\tau)=\frac{2a_2Gm}{\pi k}\int_0^{\infty}\frac{\sin qx}{q}\tau^{\alpha}\left[E_{\alpha,\beta}\left(\frac{-q^2a_3}{pr}\tau^{\alpha}\right)-E_{\alpha,\beta}\left(-a_1q^2\tau^{\alpha}\right)\right]\sin qx\,dq,$$

$$\mathrm{d}(\mathrm{x},\tau)=\frac{2a_4M}{\pi k}\int_0^{\infty}\frac{\sin qx}{q}\tau^{\alpha}\left[E_{\alpha,\beta}\left(\frac{-q^2a_3}{pr}\tau^{\alpha}\right)-E_{\alpha,\beta}\left(-a_1q^2\tau^{\alpha}\right)\right]\sin qx\,dq,$$

where, $K=\pi\,\mathrm{Pr}\left(a_1-\frac{1}{\mathrm{Pr}}\right)$,

$$v(\mathrm{x},\tau)=\mathrm{a}(\mathrm{x},\tau)+\mathrm{b}(\mathrm{x},\tau)+c(\mathrm{x},\tau)-d(\mathrm{x},\tau). \tag{19}$$

2.5. Nusselt number

From the fluid temperature, heat flow rate can be computed from the non-dimensional

$$\text{form } Nu=-L^{-1}\left[\left(\frac{\partial\bar{\theta}(\mathrm{x},\mathrm{s})}{\partial x}\right)_{x=0}\right]=L^{-1}\left[\frac{\sqrt{s^{\alpha}\,\frac{pr}{a3}}}{s}\right]=\sqrt{\frac{pr}{a3}}\,\frac{t^{-\alpha/2}}{\Gamma(1-\alpha/2)}. \tag{20}$$

2.6. Shearwood number

From the Concentration, mass flow rate can be computed from the non-dimensional form:

$$Sh=-L^{-1}\left[\left(\frac{\partial\bar{C}(\mathrm{x},\mathrm{s})}{\partial x}\right)_{x=0}\right]=L^{-1}\left[\frac{\sqrt{s^{\alpha}\,sc\,a4}}{s}\right]=\sqrt{sc\,a4}\,\frac{t^{-\alpha/2}}{\Gamma(1-\alpha/2)}. \tag{21}$$

3. Parametric study

The fractional derivative is employed in this article to generalize the convective flow of the nanofluid. The Caputo-fractional derivative is used to fractionalize the Brinkman type fluid's governing equation. From the fractional PDEs constructed to the modelling fluid flow. The nondimensional fluid temperature, species concentration, and fluid momentum equations are solved analytically using the Fourier sine and Laplace transform methods. The results obtained from the solutions of the governing model are displayed in the form of graphs to investigate the impact of the various physical terms, such as α, M, γ, ϕ, Gr, Gm, Pr and Sc. The nanofluid physical parameters are listed in Table 1.

The velocity profiles for various Prandtl number values are shown in Figure 2. It was discovered that the velocity profiles dropped as the Prandtl number raised. The proportion of momentum to thermal diffusivity is known as the Prandtl number. Due to the direct correlation between Prandtl number and momentum diffusivity, the fluid gets thicker and more viscous with less capacity for heat conduction as Pr values increase due to that the fluid travels more slowly as a consequence. The impact of Gr on the behaviour of fluid flow is seen in Figure 3. In this case, Gr>0 stands for "plate is heated up of" and Gr <0 "plate is cooled down of". When the plate is cooled, the fluid's temperature significantly rises; conversely, heating causes the fluid to move at a much slower rate. From the curve pattern, it can be seen that when the plate's surface is cooled, fluid momentum increases in Grashof number. It explains the actual finding that the buoyant force of the species improves and is enhanced as Gr rises. As seen in Figure 4, the magnetic parameter (M) affects the velocity distribution. It has been shown that the function of M is negatively impacted by nanofluid velocity. The Lorentz force, or magnetic lines, which are produced by one of Maxwell's equations and Ohm's law, may have a stronger effect on the velocity boundary close to the plate and cause slowdowns as a result. When a magnetic field is given to an electrified, insulated nanofluid, it creates a dragging force known as the Lorentz force. The Lorentz force grows stronger as M rises, allowing the nanofluid to slow gradually. Figure 5 illustrates the impact of nanoparticle volume fraction ϕ on dimensionless velocity. The velocity of nanofluids is revealed to have an inverse relationship. The thickness of the nanofluid increases as it increases ϕ, and this results in a decrease in the fluid velocity. Adding nanoparticles to a fluid increases its density, which reduces both the boundary layer thickness as well as nanofluid velocity.

Figure 6 demonstrates the flow curves for variation in α values, it is observed that increasing the order of the fractional derivative causes an increase in the fluid momentum. Since it is true that increasing time leads to an increase in the flow field, which may explain this result. Figure 7 shows how the angle (γ) affects the velocity profile. The fluid velocity profile is shown to decrease with increasing angle. The buoyant force caused by heat diffusion has a decreasing impact as the angle of inclination increases. Figure 8 depicts the effect of volume fraction (nano-sized particle volume fraction) on fluid temperature, hence noticed that with increasing the volume fraction of nanoparticle increases the temperature profile. It is because of the physical fact that, due to an increment in the density of nanoparticles, leads to a rise in the conductivity of heat.

The temperature profiles for different values of α are shown in Figure 9 while the other parameters are held constant. The Caputo fractional parameter's rising function grows as the temperature increases. The uniqueness lies in explaining how temperature rises as the fractional operator's orders grow. Increases in order have a significant influence on time values because of the memory effect inherent in fractional operators, which leads to a large accumulation. When the order of the fractional operator is increased, it is seen that a rise in time, consequently it leads to an upturn

in fluid temperature. It's also noted that a sub diffusion in the range (0, 1). The Caputo fractional derivative sub diffusion is confirmed by the literature's conclusions when the order is changed to (0, 1). Figure 10 Increasing the value of the Prandtl number makes the fluid's thermal conductivity go down, so the temperature of the nanofluid goes down.

For different magnitudes Sc, α and ϕ, the curve patterns on the species are represented in Figures 11–13. It has been noticed that the concentration drops as a raise in Schmidt number and ϕ, but increases as α increases. Different values of a number of factors were used to calculate the non-dimensional mass and heat flow rates for the nanofluids (included in Tables 2 to 3). We see a drop in the Nusselt and Shearwood numbers as t, α rises. Increasing the Prandtl number results in a rise in the Nusselt number Nu and it drops while increasing a volume fraction of a nanoparticle. With increasing of Sc and ϕ then the Shearwood number too. Table 4 displays the comparison and reveals a high level of agreement.

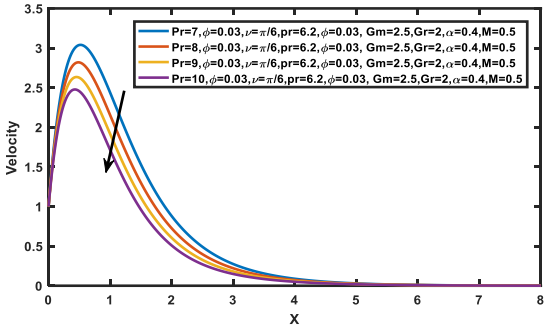

Figure 2. Variation of Pr on velocity.

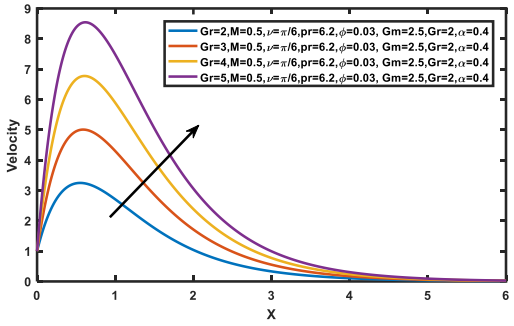

Figure 3. Variation of Gr on velocity.

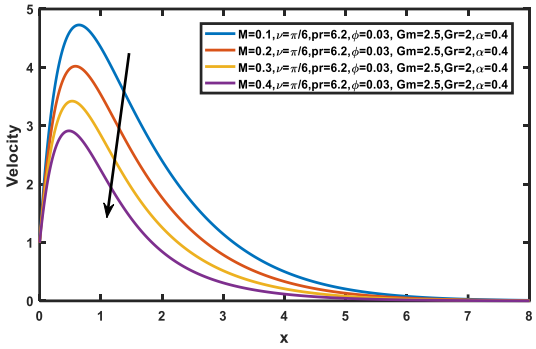

Figure 4. Variation of M on velocity.

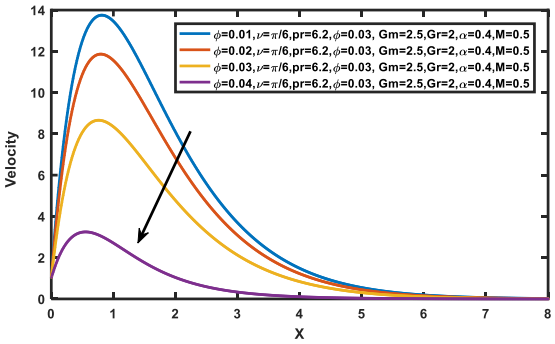

Figure 5. Variation of ϕ on velocity.

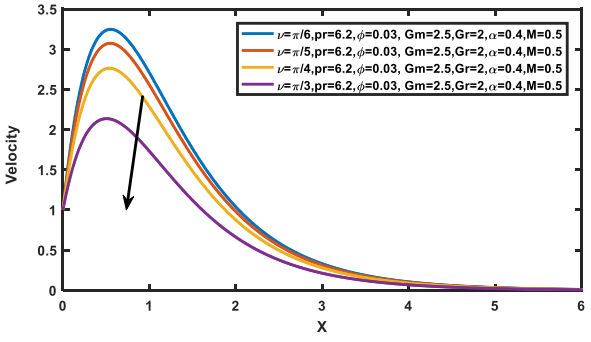

Figure 6. Variation of α on velocity.

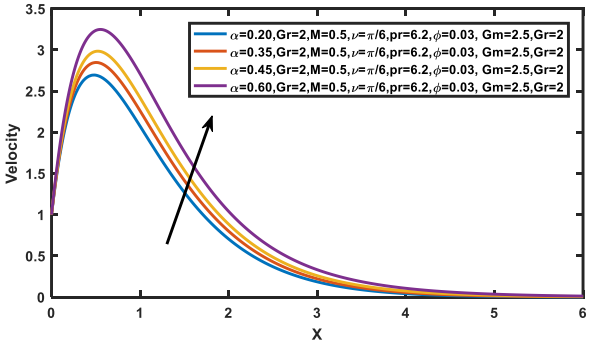

Figure 7. Variation of γ on velocity.

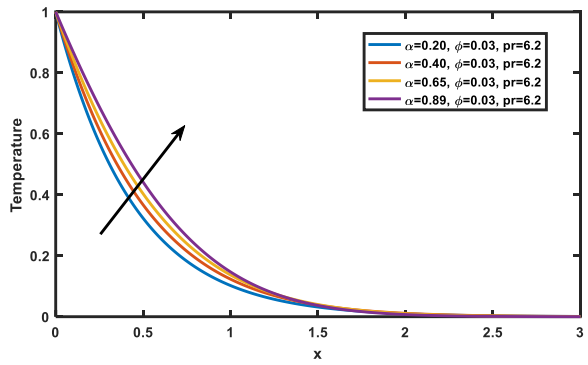

Figure 8. Variation of ϕ on temperature.

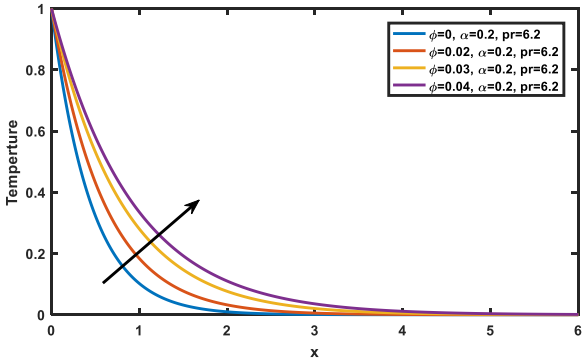

Figure 9. Variation of α on temperature.

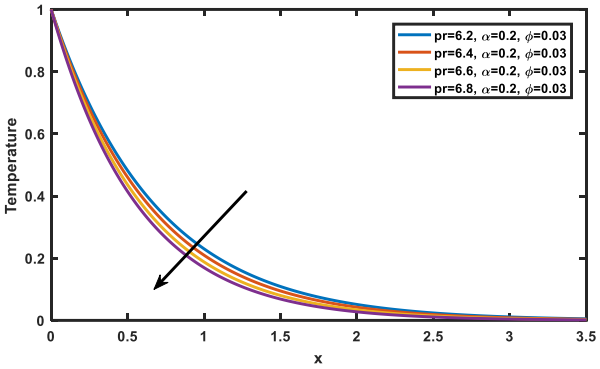

Figure 10. Variation of Pr on temperature.

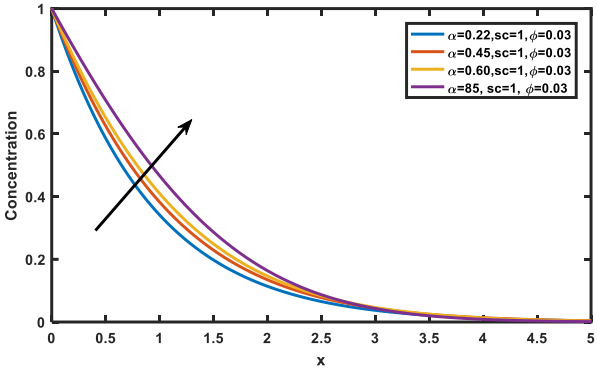

Figure 11. Variation of α on concentration.

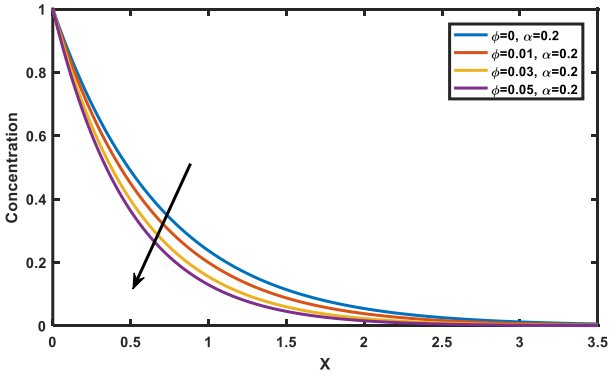

Figure 12. Variation of Sc on concentration.

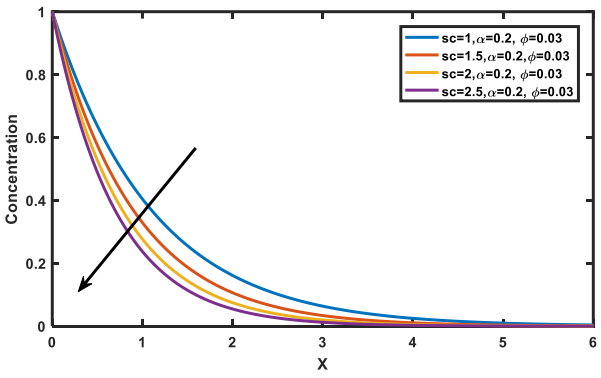

Figure 13. Variation of ϕ on concentration.

Table 1. Thermophoresis properties of water and Clay Nanoparticle [43].

Thermophysical Property	$\rho\left(kg/m^3\right)$	$C_p(J/kgK)$	$k(w/mK)$	$\beta(1/k)$
H_2O	997.1	4179	0.613	$21_{\times}10^{-5}$
Clay	6320	531.8	76.5	$1.80_{\times}10^{-5}$

Table 2. Nusselt number.

t	α	Pr	ϕ	Nu
1	0.22	6.7	0.3	1.5578490609
1.5				1.0859358139
2				0.8406373474
	0.42			0.8252379429
	0.62			0.7912402832
	0.82			0.7367901660
		6.9		0.7477061704
		7.1		0.7584650855
		7.3		0.7690735040
			0.4	0.6667779206
			0.5	0.5739573719
			0.6	0.4872590819

Table 3. Shearwood number.

T	α	Sc	ϕ	Sh
0.5	0.46	1	0.2	1.5891987144
1				0.9319338967
1.5				0.6820164329
	0.56			0.6587650874
	0.66			0.6320018337
	0.76			0.6017264546
		2		1.2034529092
		3		1.8051793638
		4		2.4069058184
			0.3	2.5730905527
			0.4	2.7792554443
			0.5	3.0445217998

Table 4. Comparison of Nusselt number when $\phi = 0$.

t	α	Pr	Nodolane sene [7]	Present result
1	0.84	12	2.2539	2.25672
1		18	2.7605	2.7564
	0.94		3.1875	3.1645

Limiting case: $\alpha \to 1$

Temperature and concentration for classical case

The temperature and Concentration expression corresponding to $\alpha \to 1$ in Eqs (2) and (3) reduces to the following expression

$$(\rho_{cp})_{nf} \frac{\partial T'(x,t)}{\partial t'} = a_3 \frac{\partial^2 T'}{\partial x'^2}, \tag{22}$$

$$\frac{\partial C}{\partial t} = a_5 \frac{1}{sc} \frac{\partial^2 C}{\partial x^2}. \tag{24}$$

By using Laplace and Inverse Laplace transformation we will get the solution for the above equations:

$$\theta(x,\tau) = erfc\left(\frac{x\sqrt{\Pr}}{2\sqrt{ta_3}}\right),$$

$$\mathrm{C}(x,\tau) = erfc\left(\frac{x\sqrt{sc}}{2\sqrt{ta_5}}\right),$$

where $erfc$ is a Gaussian error function.

4. Conclusions

This article examines the effects of MHD on electrically conducting incompressible viscous nanofluid flowing freely over an inclined plate. The analytical solutions for nanofluid with Clay nanoparticles are obtained using Caputo fractional derivates. A Caputo fractional model is developed using a combination of two popular methods in this research. The Laplace transform for time derivatives and the sine Fourier Transform for special derivative methods for each the governing equations of the flow field. The main findings of this analysis are:

- As the magnetic field and angle of inclination are increased, the velocity profile for nanofluids decreases.
- The velocity, temperature and Concentration profiles show an increasing behaviour for increasing values α.
- The concentration boundary layer reduces as an increase in nanoparticles volume fraction, but the energy boundary layer and momentum boundary layer are increased for the nanofluid.
- Temperature decreases with increasing of Pr.
- For nanofluid the velocity profiles are increased as an increase of Gr.
- Concentration decreases with an increase in Schmidt number Sc.
- As the fractional parameter is increased, the Nu and Sh values are reduced.

Acknowledgements

Taif University Researchers Supporting Project number (TURSP-2020/154), Taif University, Taif, Saudi Arabia.

Conflict of interest

The authors declare that they have no competing interests.

References

1. S. U. S. Choi, J. A. Eastman, *Enhancing thermal conductivity of fluids with nanoparticles*, Conference: International mechanical engineering congress and exhibition, San Francisco, CA, 1995, 12–17.
2. V. W. Kaufui, D. L. Omar, Applications of nanofluids: Current and future, *Adv. Mech. Eng.*, **11** (2010), 105–132.
3. O. Mahian, L. Kolsi, M. Amani, P. Estellé, G. Ahmadi, C. Kleinstreuer, et al., Recent advances in modeling and simulation of nanofluid flows-Part I: Fundamentals and theory, *Phys. Rep.*, **790** (2019), 1–48. https://doi.org/10.1016/j.physrep.2018.11.004
4. J. A. Eastman, U. S. Choi, S. P. Li, L. J. Thompson, S. Lee, *Enhanced thermal conductivity through the development of nanofluids*, Cambridge University Press, **457** (1996). https://doi.org/10.1557/PROC-457-3
5. J. A. Eastman, U. S. Choi, S. P. Li, W. Yu, L. J. Thompson, Anomalously increased effective thermal conductivities of ethylene glycol-based nanofluids containing copper nanoparticles, *Appl. Phys. Lett.*, **78** (2001), 718–720. https://doi.org/10.1063/1.1341218
6. N. A. Sheikh, D. L. C. Ching, H. Sakidin, I. Khan, Fractional model for the flow of Brinkman-type fluid with mass transfer, *J. Adv. Res. Fluid Mech. Therm. Sci.*, **93** (2022), 76–85. https://doi.org/10.37934/arfmts.93.2.7685
7. N. Sene, Analytical investigations of the fractional free convection flow of Brinkman type fluid described by the Caputo fractional derivative, *Results Phys.*, **37** (2022), 105555. https://doi.org/10.1016/j.rinp.2022.105555
8. M. M. Ghalib, A. A. Zafar, M. Farman, A. Akgül, M. O. Ahmad, A. Ahmad, Unsteady MHD flow of Maxwell fluid with Caputo-Fabrizio non-integer derivative model having slip/non-slip fluid flow and Newtonian heating at the boundary, *Indian J. Phys.*, **96** (2022), 127–136. https://doi.org/10.1007/s12648-020-01937-7
9. N. Iftikhar, S. T. Saeed, M. B. Riaz, Fractional study on heat and mass transfer of MHD Oldroyd-B fluid with ramped velocity and temperature, *J. Comput. Method. Appl. Math.*, **10** (2021), 372–395. https://doi.org/10.22034/cmde.2021.39703.1739
10. A. Raza, S. U. Khan, K. Al-Khaled, M. I. Khan, A. U. Haq, F. Alotaibi, et al., A fractional model for the kerosene oil and water-based Casson nanofluid with inclined magnetic force, *Chem. Phys. Lett.*, **787** (2022), 139277. https://doi.org/10.1016/j.cplett.2021.139277
11. I. Podlubny, *Fractional differential equations*, Academic Press, San Diego, 1991. Available from: http://www.sciepub.com/reference/3051.
12. N. Sene, Fractional SIRI model with delay in context of the generalized Liouville-Caputo fractional derivative, *Math. Model. Comput.*, 2020, 107–125.
13. M. A. Imran, N. A. Shah, I. Khan, M. Aleem, Applications of non-integer Caputo time fractional derivatives to natural convection flow subject to arbitrary velocity and Newtonian heating, *Neural Comput. Appl.*, **30** (2018), 1589–1599. https://doi.org/10.1007/s00521-016-2741-6
14. I. Khan, N. A. Shah, D. Vieru, Unsteady flow of generalized Casson fluid with fractional derivative due to an infinite plate, *Eur. Phys. J. Plus*, **131** (2016), 1–12. https://doi.org/10.1140/epjp/i2016-16181-8
15. A. Khalid, I. Khan, A. Khan, S. Shafie, Unsteady MHD free convection flow of Casson fluid past over an oscillating vertical plate embedded in a porous medium, *Eng. Sci. Technol. Int. J.*, **18** (2015), 309–317. https://doi.org/10.1016/j.jestch.2014.12.006

16. F. Ali, M. Saqib, I. Khan, N. A. Sheikh, Application of Caputo-Fabrizio derivatives to MHD free convection flow of generalized Walters'-B fluid model, *Eur. Phys. J. Plus.*, **131** (2016), 1–10. https://doi.org/10.1140/epjp/i2016-16377-x
17. S. Qureshi, A. Yusuf, A. A. Shaikh, M. Inc, Transmission dynamics of varicella zoster virus modeled by classical and novel fractional operators using real statistical data, *Phys. A*, **534** (2019), 122149. https://doi.org/10.1016/j.physa.2019.122149
18. F. Ali, N. A. Sheikh, I. Khan, M. Saqib, Magnetic field effect on blood flow of Casson fluid in axisymmetric cylindrical tube: A fractional model, *J. Magn. Magn. Mater.*, **423** (2017), 327–336. https://doi.org/10.1016/j.jmmm.2016.09.125
19. B. Steinfeld, J. Scott, G. Vilander, L. Marx, M. Quirk, J. Lindberg, K. Koerner, The role of lean process improvement in implementation of evidence-based practices in behavioral health care, *J. Behav. Health Ser. R.*, **42** (2015), 504–518. https://doi.org/10.1007/s11414-013-9386-3
20. M. Caputo, M. Fabrizio, A new definition of fractional derivative without singular kernel, *Prog. Fract. Differ. Appl.*, **1** (2015), 73–85. http://dx.doi.org/10.12785/pfda/010201
21. B. S. T. Alkahtani, A. Atangana, Analysis of non-homogeneous heat model with new trend of derivative with fractional order, *Chaos Soliton. Fract.*, **89** (2016), 566–571. https://doi.org/10.1016/j.chaos.2016.03.027
22. K. Diethelm, N. J. Ford, A. D. Freed, Y. Luchko, Algorithms for the fractional calculus: a selection of numerical methods, *Comput. Method. Appl. M.*, **194** (2005), 743–773. https://doi.org/10.1016/j.cma.2004.06.006
23. S. Aman, I. Khan, Z. Ismail, M. Z. Salleh, I. Tlili, A new Caputo time fractional model for heat transfer enhancement of water based graphene nanofluid: An application to solar energy, *Result. Phys.*, **9** (2018), 1352–1362. https://doi.org/10.1016/j.rinp.2018.04.007
24. N. A. Shah, A. Wakif, R. Shah, S. J. Yook, B. Salah, Y. Mahsud, et al., Effects of fractional derivative and heat source/sink on MHD free convection flow of nanofluids in a vertical cylinder: A generalized Fourier's law model, *Case Stud. Therm. Eng.*, **28** (2021), 101518. https://doi.org/10.1016/j.csite.2021.101518
25. Al. Raza, I. Khan, S. Farid, C. A. My, A. Khan, H. Alotaibi, Non-singular fractional approach for natural convection nanofluid with Damped thermal analysis and radiation, *Case Stud. Therm. Eng.*, **28** (2021), 101373. https://doi.org/10.1016/j.csite.2021.101373
26. M. D. Ikram, M. I. Asjad, A. Akgül, D. Baleanu, Effects of hybrid nanofluid on novel fractional model of heat transfer flow between two parallel plates, *Alex. Eng. J.*, **60** (2021), 3593–3604. https://doi.org/10.1016/j.aej.2021.01.054
27. M. B. Riaz, J. Awrejcewicz, D. Baleanu, Exact solutions for thermomagetized unsteady non-singularized jeffrey fluid: Effects of ramped velocity, concentration with newtonian heating, *Result. Phys.*, **26** (2021), 104367. https://doi.org/10.1016/j.rinp.2021.104367
28. A. U. Rehman, M. B. Riaz, A. Akgül, S. T. Saeed, D. Baleanu, Heat and mass transport impact on MHD second-grade fluid: A comparative analysis of fractional operators, *Heat Transf.*, **50** (2021), 7042–7064. https://doi.org/10.1002/htj.22216
29. J. Zhang, A. Raza, U. Khan, Q. Ali, A. Zaib, W. Weera, et al., Thermophysical study of Oldroyd-B hybrid nanofluid with sinusoidal conditions and permeability: A prabhakar fractional approach, *Fractal Fract.*, **6** (2022), 357. https://doi.org/10.3390/fractalfract6070357
30. M. B. Riaz, A. U. Rehman, J. Awrejcewicz, F. Jarad, Double diffusive magneto-free-convection flow of Oldroyd-B fluid over a vertical plate with heat and mass flux, *Symmetry*, **14** (2022), 209. https://doi.org/10.3390/sym14020209
31. H. Elhadedy, H. Abass, A. Kader, S. Mohamed, A. Latif, Investigating heat conduction in a

sphere with heat absorption using generalized Caputo fractional derivative, *Heat Transf.*, **50** (2021), 6955–6963. https://doi.org/10.1002/htj.22211
32. A. H. A. Kader, S. Mohamed, A. Latif, D. Baleanu, Studying heat conduction in a sphere considering hybrid fractional derivative operator, *Therm. Sci.*, **26** (2022), 1675–1683. https://doi.org/10.2298/TSCI200524332K
33. M. Khan, A. Rasheed, M. S. Anwar, Z. Hussain, T. Shahzad, Modelling charge carrier transport with anomalous diffusion and heat conduction in amorphous semiconductors using fractional calculus, *Phys. Scr.*, **96** (2021), 045204. https://doi.org/10.1088/1402-4896/abde0f
34. M. Irfan, K. Rafiq, M. S. Anwar, M. Khan, W. A. Khan, K. Iqbal, Evaluating the performance of new mass flux theory on Carreau nanofluid using the thermal aspects of convective heat transport, *Pramana*, **95** (2021), 1–9. https://doi.org/10.1007/s12043-021-02217-7
35. I. Ali, A. Rasheed, M. S. Anwar, M. Irfan, Z. Hussain, Fractional calculus approach for the phase dynamics of Josephson junction, *Chaos Soliton. Fract.*, **143** (2021), 110572. https://doi.org/10.1016/j.chaos.2020.110572
36. Z. Hussain, A. Hussain, M. S. Anwar, M. Farooq, Analysis of Cattaneo-Christov heat flux in Jeffery fluid flow with heat source over a stretching cylinder, *J. Therm. Anal. Calorim.*, **147** (2022), 3391–3402. https://doi.org/10.1007/s10973-021-10573-0
37. N. S. Akbar, D. Tripathi, Z. H. Khan, O. A. Bég, A numerical study of magnetohydrodynamic transport of nanofluids over a vertical stretching sheet with exponential temperature-dependent viscosity and buoyancy effects, *Chem. Phys. Lett.*, **661** (2016), 20–30. https://doi.org/10.1016/j.cplett.2016.08.043
38. N. Sene, Analytical solutions of a class of fluids models with the Caputo fractional derivative, *Fractal Fract.*, **6** (2022), 35. https://doi.org/10.3390/fractalfract6010035
39. S. Aman, I. Khan, Z. Ismail, M. Z. Salleh, I. Tlili, A new Caputo time fractional model for heat transfer enhancement of water based graphene nanofluid: An application to solar energy, *Result. Phys.*, **9** (2018), 1352–1362. https://doi.org/10.1016/j.rinp.2018.04.007
40. T. Anwar, P. Kumam, Z. Shah, W. Watthayu, P. Thounthong, Unsteady radiative natural convective MHD nanofluid flow past a porous moving vertical plate with heat source/sink, *Molecules,* **25** (2020), 854. https://doi.org/10.3390/molecules25040854
41. F. Shen, W. C. Tan, Y. H. Zhao, T. Masuoka, The Rayleigh-Stokes problem for a heated generalized second grade fluid with fractional derivative model, *Nonlinear Anal.-Real*, **7** (2006), 1072–1080. https://doi.org/10.1016/j.nonrwa.2005.09.007
42. A. Raza, S. U. Khan, S. Farid, M. I. Khan, T. C. Sun, A. Abbasi, et al., Thermal activity of conventional Casson nanoparticles with ramped temperature due to an infinite vertical plate via fractional derivative approach, *Case Stud. Therm. Eng.*, **27** (2021), 101191. https://doi.org/10.1016/j.csite.2021.101191
43. S. Aman, I. Khan, Z. Ismail, M. Z. Salleh, Applications of fractional derivatives to nanofluids: Exact and numerical solutions, *Math. Model. Nat. Pheno.*, **13** (2018), 2. https://doi.org/10.1051/mmnp/2018013